J Fluoresc (2014) 24:885–894
DOI 10.1007/s10895-014-1366-3

ORIGINAL PAPER

Fret Studies of Conformational Changes in Heparin-Binding Peptides

Eduardo Sérgio de Souza · Alberto H. Katagiri · Luiz Juliano · Maria Aparecida Juliano · Daniel Carvalho Pimenta · Amando Siuiti Ito

Received: 4 October 2013 / Accepted: 5 February 2014 / Published online: 11 April 2014

Abstract FRET (Förster Resonance Energy Transfer) was applied to study structural properties of heparin-binding peptides containing the sequence XBBBXXBX where 'X' represents hydropathic or uncharged and 'B' represents basic amino acids. Internally quenched fluorogenic peptides were synthesized containing the fluorescent donor oaminobenzoic acid (o-Abz) and the acceptor dinitrophenyl ethylenediamine (Eddnp) group. Using the CONTIN computational package, distance distributions were recovered from time resolved fluorescence data, associated to end-to-end distances of the peptides. The peptides containing three or four repeat units have random structure in aqueous medium, and the interaction with low molecular weight heparin stabilized short end-to end distances. Experiments in water/trifluoroethanol (TFE) mixtures showed changes in distance distributions compatible with compact conformations stabilized above 40 % volume content of TFE in the mixture. Similar changes in distance distributions were also observed for the peptides in interaction with SDS micelles in aqueous suspensions and circular dichroism data revealed alpha-helix formation in the peptides in interaction with heparin, SDS micelles or the co-solvent TFE. The process is dependent on electrostatic and hydrogen bond interactions and the end-to-end distances obtained are smaller than expected for the peptides in linear α-helix conformation, indicating the occurrence of structural arrangements leading to additional decrease in the distances.

Keywords Glycosaminoglican · Cardin motif peptides · Time resolved fluorescence · Forster resonant energy transfer · Intramolecular distance · Internally quenched fluorogenic peptides · Heparin

E. S. de Souza (✉)
Departamento de Física, Universidade Federal de Goiás, Campus Catalão, Av. Dr. Lamartine Pinto de Avelar, 1120, 75704-020 Catalão, GO, Brazil
e-mail: souza.es@gmail.com

A. H. Katagiri
Instituto de Física, Universidade de São Paulo, Rua do Matão, Travessa R, 187, Cidade Universitária, 05508-090 São Paulo, SP, Brazil

L. Juliano · M. A. Juliano
Departamento de Biofísica, Escola Paulista de Medicina, Universidade Federal de São Paulo, Rua Três de Maio, 100, 04044-020 São Paulo, SP, Brazil

D. C. Pimenta
Laboratório de Bioquímica e Biofísica, Instituto Butantan, Avenida Vital Brasil, 1500, 05503-900 São Paulo, SP, Brazil

A. S. Ito
Faculdade de Filosofia Ciências e Letras de Ribeirão Preto, Universidade de São Paulo, Av. Bandeirantes 3900, 14040-901 Ribeirão Preto, SP, Brazil

Introduction

Glycosaminoglycans (GAGs), linear polysaccharides consisting of a repeating disaccharide unit, bind to a large number of proteins, playing an essential role in the regulation of various physiological processes [1]. Heparin, a glycosaminoglycan, is a linear polymer consisting of repeating units of 1-4-linked pyranosyluronic acid and glucosamine, widely used as an anticoagulant drug based on its ability to accelerate the rate at which antithrombin inhibits serine proteases thrombin and factor Xa in the blood coagulation cascade [2–5]. Undesirable side effects of heparin, such as heparin-induced thrombocytopenia (HIT) led to the development of low-molecular-weight (LMW) heparin fractions [6–8].

Protamine, a heterogeneous, sometimes toxic protein mixture is commonly used to neutralize the anticoagulant activity of heparin in humans [9, 10]. Research on synthetic heparin-binding peptides aimed to neutralize the effects of heparin as

an alternative to protamine has been tried because of the side effects of this mixture of arginine-rich basic peptides [11–14]. Verrechio and co-workers [15] described the design and characterization of high affinity heparin binding peptides synthesized based in the heparin-binding consensus sequences XBBXBX and XBBBXXBX (where 'X' represents hydropathic or uncharged amino acids, and 'B' represents basic amino acids) [16]. Spectroscopic studies using CD and NMR techniques showed structural changes in peptides containing XBBBXXBX sequences from random coil to α-helix conformation due to interaction with heparin as well as in the presence of cosolvents like trifluoroethanol (TFE) [17] or lipid aggregates [18]. It was observed that arginine and lysine rich peptides have high affinity to heparin, and structural changes are associated to ionic interactions and hydrogen bond formation [19, 20]. Molecular modeling and computational simulations stressed that the spatial arrangement of charged residues have important role in the interaction between peptides and heparin [19, 21].

Among the several fluorescence spectroscopy techniques, those based on energy transfer have been employed to study biomacromolecules and processes involving internal structure of proteins. Peptides containing a fluorescent group (donor) at one end and a quencher group (acceptor) at the other end have been synthesized and used as substrates for protease assays, examining the increase in fluorescence with the progression of enzymatic hydrolysis due to the elimination of donor-acceptor intramolecular energy transfer [22, 23]. *Ortho*-Aminobenzoic acid (*o*-Abz) is a small fluorescent probe, with size and structure comparable to those of natural amino acids, and has been used as a convenient donor group, forming a donor-acceptor pair with N-[2,4-dinitrophenyl]-ethylenediamine (EDDnp) in internally quenched fluorogenic (IQF) peptides, employed for example in the investigation of proteases as human tissue kallikrein [24, 25]. The spectroscopic characteristics of *o*-Abz bound to amino acids and small peptides have been studied in aqueous medium [26] and in different solvents [27, 28], as well as in interaction with amphiphilic aggregates like micelles and vesicles [29–31].

Time-resolved fluorescence data were used in FRET studies to obtain intramolecular distances. The conformacional flexibility of IQF peptides was investigated through the analysis of the complex decay kinetics of peptides labeled with donor and acceptor groups, and the program CONTIN was developed to recover donor-acceptor distance distribution f(r) [32–35]. In studies about the heparin binding peptides, IQF peptides were synthesized base on the sequence published by Verrechio and co-workers [15] and their interaction with LMW heparin was studied by different spectroscopic techniques, including time resolved fluorescence [36]. Among the peptides investigated, the one with sequence *o*-Abz-(ARKKAAKA)$_4$-Q-EDDnp (hereafter written as RKK-4) showed higher affinity to LMW heparin compared to the shorter peptide with sequence *o*-Abz-(ARKKAAKA)$_3$-Q-EDDnp (hereafter called RKK-3). It was observed by circular dichroism spectroscopy that the conformation of the long peptide changed from random coil in buffer to 89.6 % alpha-helix content after addition of LMW heparin [36].

In this work we investigated the conformational changes in the IQF peptides RKK-4 and RKK-3 induced by interaction with heparin, by time-resolved fluorescence spectroscopy. The decay kinetics of the peptides was fitted to multi-exponential curves and the program CONTIN was employed to recover the donor-acceptor distance distribution f(r) from the experimental decays, both in buffer solution as in interaction with LMW heparin. In order to evaluate the contribution due to electrostatic interactions, experiments were performed also in the presence of anionic micelles of sodium dodecyl sulfate (SDS) and the influence of hydrogen bond formation was investigated in buffer solution containing trifluoroethanol as co-solvent. We observed that the conformational changes in the interaction of peptides with heparin are dependent on electrostatic and hydrogen bond interactions, with further occurrence of structural arrangements in the peptide-heparin complexes, leading to additional decreases in the intramolecular distances.

Materials and Methods

Reagents

Low-molecular-mass (LMW) heparin (4500 Da, modal mass) was purchased from Aventis (Parsippany, NJ, U.S.A.). All chemicals used were from Sigma-Aldrich (St. Louis, MO, U.S.A.) or from Calbiochem (San Diego, CA, U.S.A.).

Synthetic Substrates

All the IQF peptides contained EDDnp attached to glutamine, a necessary result of the solid-phase peptide synthesis strategy employed, as described previously [37]. An automated bench-top simultaneous multiple solid-phase peptide synthesizer (PSSM 8 system, from Shimadzu) was used for the solid-phase synthesis of all the peptides using the fluoren-9-ylmethoxycarbonyl ('Fmoc') procedure. The final deprotected peptides were purified by binary semi-preparative HPLC using an Econosil C-18 column (10 μm, 22.5 mm× 250 mm) and solvents A [trifluoroacetic acid/H_2O(1:1000, v/v)], and B [trifluoroacetic acid/acetonitrile/H_2O (1:900:100, by vol.)]. The column was eluted at a flow rate of 5 ml/min with a 10±60 % gradient of solvent B over the course of 30 to 45 min, depending on the sequence. Analytical HPLC was performed using a binary HPLC system from Shimadzu with a SPD-10AV Shimadzu UV-visible light detector and a Shimadzu RF-10AXL fluorescence detector,

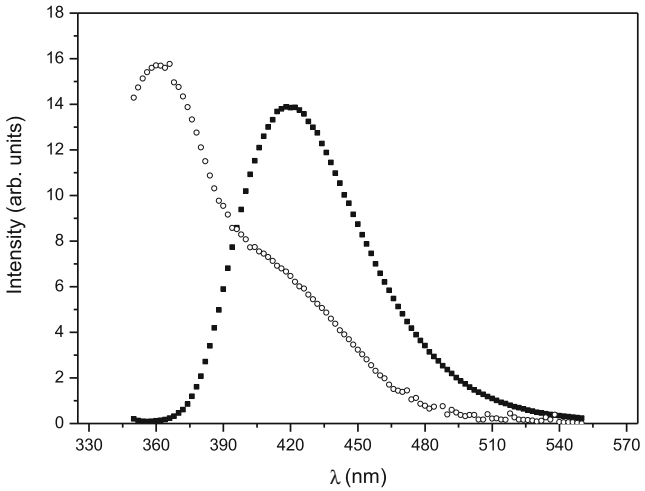

Fig. 1 Spectral superposition of KK-Q absorption (*white circle*) and KK-A emission (*black square*), with excitation at 310 nm, in phosphate buffer 10 mM, pH 7.4, 20 °C, containing equimolar concentration of heparin 30 μM. Spectra are normalized to unity at absorption or emission peaks

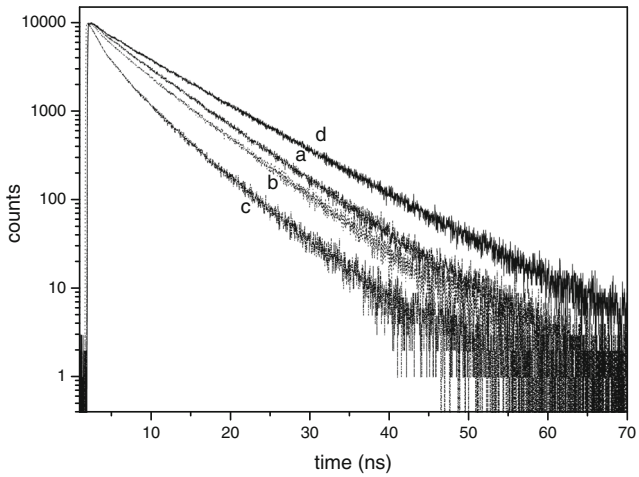

Fig. 2 Fluorescence decay curves for RKK-3 peptide 30 μM in (*a*) Phosphate Buffer, (*b*) TFE and (*c*) LMW heparin. Curve (*d*) shows the decay, in phosphate buffer, of the peptide KK-A containing the donor group without acceptor

coupled with an Ultrasphere C-18 column (5 μm, 4.6 mm× 150 mm) that was eluted with solvent systems A and B at a flow rate of 1 ml/min and a 10–80 % gradient of B over 20 min. The HPLC column eluates were monitored by their absorbance at 220 nm and by fluorescence emission at 420 nm following excitation at 320 nm. The molecular mass and purity of synthesized peptides were checked by matrix-assisted laser-desorption-time-of-flight (MALDI-TOF) MS (TofSpec-E, Micromass, Manchester, U.K.) and/or peptide sequencing using a protein sequencer PPSQ-23 (Shimadzu Tokyo, Japan).

Measurements

Stock solutions of peptides were prepared in water. Measurements were made diluting the stock solution with phosphate buffer 10 mM, pH 7.4, or TFE to final peptide concentrations between 2×10^{-5} M and 4×10^{-5} M. In TFE/water mixture experiments, pH was adjusted to 7.4 with addition of NaOH.

Optical absorption measurements were performed using an HP 8452 A diode array spectrophotometer. For steady-state fluorescence experiments we employed a Fluorolog 3 Jobin Yvon-Spex spectrometer. Excitation and emission slits of 1- or 2-nm bandpass were used, depending on the fluorescence intensity of the sample. *o*-Abz emission quantum yield was determined using as reference the value of 0.60 reported for the fluorophore in ethanol [38]. The temperature was controlled using a Forma Scientific 2006 thermal bath. Time-resolved experiments were performed using an apparatus based on the time-correlated single photon counting method. The excitation source was a Tsunami 3950 Spectra Physics titanium-sapphire laser, pumped by a 2060 Spectra Physics argon laser. The repetition rate of the 5 ps pulses was set to 400 or 800 kHz using the pulse picker 3980 Spectra Physics. The laser was tuned to give output at 930 or 888 nm, and a third harmonic generator BBO crystal (GWN-23PL Spectra Physics) gave, respectively, the 310 or 296 nm excitation pulses that were directed to an Edinburgh FL900 spectrometer. The L-format configuration of the spectrometer allowed detection of the emission at a right angle from the excitation, and for anisotropy measurements it was employed a Glan Thompson polarizer in the emission beam and a Soleil Babinet compensator in the excitation beam. The emission wavelength was selected by a monochromator, and emitted photons were detected by a refrigerated Hamamatsu R3809U microchannel plate photomultiplier. The FWHM of the instrument response function was typically 45 ps, determined with a time resolution of 6.0 ps per channel, and measurements were made using time resolution of 12 ps per channel. Software provided by Edinburgh Instruments was used to analyze the decay curves, and the adequacy of the multi-exponential decay fitting was judged by inspection of the plots of weighted residuals and by statistical parameters such as reduced χ^2.

Table 1 Typical values of refractive index (**n**), quantum yield (ϕ_d), superposition integral (**J**) and Forster distance ($\boldsymbol{R}_0$) for the pair donor (KK-A, 30 μM) and acceptor (KK-Q, 30 μM) in phosphate buffer pH 7.4, in buffer solution containing with equimolar concentration of heparin or SDS 30 mM, and in TFE. Estimated errors in J value, 5 % and in R_o, 10 %

	n	ϕ_d	J (M^{-1} cm^3)	$\boldsymbol{R}_0$ (Å)
Phosphate buffer	1.334±0.001	0.30±0.01	5.13×10^{-15}	25.7
LMW heparin	1.334±0.001	0.35±0.01	4.93×10^{-15}	25.8
SDS	1.334±0.001	0.32±0.01	4.48×10^{-15}	25.4
TFE	1.291±0.001	0.34±0.01	7.36×10^{-15}	28.0

Table 2 Fluorescence decay parameters for 30 μM peptide KK-A in phosphate buffer pH 7.4, in buffer solution containing with equimolar concentration of heparin or SDS 30 mM, and in TFE. Excitation 310 nm, emission 420 nm, temperature 25°C. <τ>, mean lifetimes calculated as a simple weighted average value from the individual lifetimes (τ_i) and the corresponding normalized pre-exponential factors (a_i). Deviations in a_i: ±0.01

	τ_1(ns)	τ_2(ns)	τ_3(ns)	a_1	a_2	a_3	<τ>(ns)
Buffer	8.6±0.1	3.10±0.05	–	0.83	0.17	–	8.2±0.1
LMW heparin	9.3±0.1	3.57±0.05	–	0.76	0.24	–	8.6±0.1
SDS	10.0±0.1	4.56±0.05	0.37±0.01	0.65	0.12	0.23	9.5±0.1
TFE	8.8±0.1	4.47±0.05	0.92±0.05	0.69	0.16	0.15	8.2±0.1

Computation

In the Förster resonant energy transfer (FRET) the donor (D) emission is quenched by the presence of an acceptor (A) molecule, in a process originated from dipole-dipole interaction between the dipole moments of the two chromophores. The energy transfer adds a non-radiative path for the deexcitation of the donor emission and the decay rate gains an additional term with rate constant (k_{Fret}), dependent on the D-A distance (r), given by

$$k_{FRET} = \frac{9000(ln10)\kappa^2\phi_d}{128\pi^5 n^4 N_0 r^6 \tau_d}\int_0^\infty F_d(\lambda)\varepsilon_a(\lambda)\lambda^4 d\lambda \qquad (1)$$

where τ_d is the lifetime without FRET, n is the refractive index of the medium Φ_d is the quantum yield of the donor, N_o is Avogadro's number and κ is the orientational term dependent on the relative angles between dipoles moments from donor and acceptor. A mean value for the orientational term was set equal to 2/3 and the integral present in the equation represents the spectral superposition between donor's emission $F_d(\lambda)$ and acceptor's extinction coefficient for absorption $\varepsilon_a(\lambda)$.

The fluorescence decay of the donor, becomes faster in the presence of the acceptor and the intensity decay in the case of a fixed D-A distance is written

Table 3 Values of quantum yield (ϕ_d), superposition integral (**J**) and Forster distance ($\boldsymbol{R}_0$) for the pair donor (KK-A) and acceptor (KK-Q) in phosphate buffer pH 7.4 with equimolar concentration (Cp) in solution containing heparin at different concentrations (Ch). Estimated errors in J value, 5 % and in R_o, 10 %

Ch/Cp	Ch(μM)	Cp(μM)	ϕ_d	J($M^{-1}cm^3$)	R_0 (Å)
0.00	0.00	34.00	0.30±0.01	5.13E-11	25.7
0.15	5.00	32.45	0.23±0.01	4.97E-11	24.5
0.47	15.00	31.68	0.34±0.01	5.01E-11	26.3
0.65	20.00	30.91	0.36±0.01	4.99E-11	26.1
0.83	25.00	30.14	0.34±0.01	4.85E-11	26.4
1.02	30.00	29.36	0.38±0.01	4.93E-11	26.1
1.44	40.00	27.82	0.35±0.01	4.92E-11	25.4

$$I(t) = I_0 exp\left[\left(-\frac{1}{\tau_d} - \frac{R_0^6}{\tau_d r^6}\right)t\right] \qquad (2)$$

where the Förster distance R_o is calculated from

$$R_0^6 = \frac{9000(ln10)\kappa^2\phi_d}{128\pi^5 n^4 N_0}\int_0^\infty F_d(\lambda)\varepsilon_a(\lambda)\lambda^4 d\lambda \qquad (3)$$

However, this equation fails to fit the experimental decay when more than one distance is present during the time decay of the fluorophore. If the distance distribution can be represented by $f(r)$, it can be recovered from the experimental data by the use of the CONTIN program [39] that inverts general systems of linear algebraic equations of the type

$$y(t_k) = \int_a^b f(r)K(r,t_k)dr + \sum_{j=1}^{N_L}\beta_j L_j(t_k), k = 1, \ldots\ldots N_y \qquad (4)$$

In this work, $y(t_k)$ corresponds to the experimentally observed intensity of fluorescence at the instant t_k. The distance distribution function $f(r)$ is recovered within a chosen interval for r, initially set between $R_0/2$ and $2R_0$, divided in N equally spaced intervals, and the integral is converted, by numerical integration, to a summation in r_j. The function inside the integral is then written as $K(r_j, t_k)$ and corresponds to Eq. (2) written for the instant t_k deconvoluted from the instrument response function, and assumed to be valid for each distance r_j within the chosen interval. The second term in Eq. (4) accounts for impurities that may be present contributing to the decay profile. The program recovers the parameter β_j corresponding to the contribution L_{kj} of the jth impurity to the fluorescence intensity at the instant t_k. In the analysis we also imposed the constraint of non-negativity for the distribution function. The best solution was found using the weighted least-squares method with the employment of a regularizer based on the principles of parsimony [39].

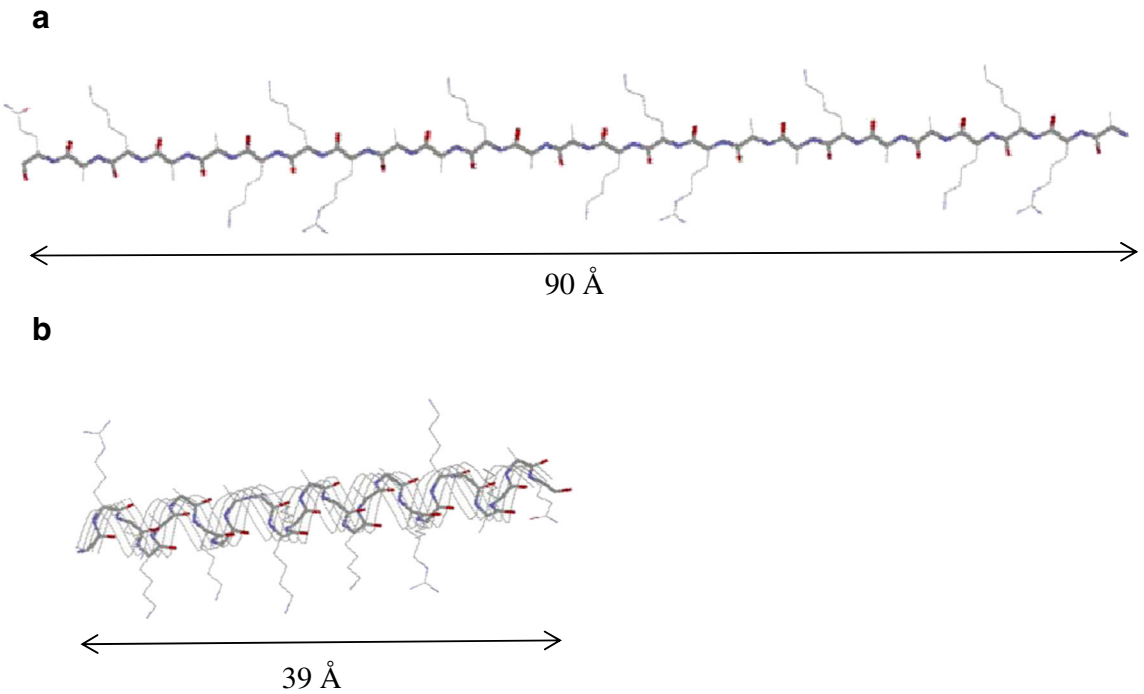

Fig. 3 Comparison between two possible conformations of peptide RKK-3, determined by molecular modeling using HyperChem software (Hypercube Inc., Gainesville, FL, U.S.A., http://www.hyper.com) extended conformation (**a**), (**b**) all α-helix conformation

Results and Discussion

The spectral characteristics of *o*-Abz and EDDnp free and bound to peptides have been previously studied [33–35]. Internally quenched fluorogenic peptides Abz-$(AKKARA)_n$-Q-EDDnp and Abz-$(ARKKAAKA)_n$-Q-EDDnp, where *n* varied from 1 to 4, containing *o*-Abz as donor and EDDnp as acceptor, were studied by Pimenta and co-workers [36]. The emission of the peptide containing only the donor (Abz-AKKARAAKKARAAKKARAQ-NH2, hereafter named KK-A), shows spectral superposition with the absorption of the peptide containing only the acceptor (AKKARAAKKARAAKKARAQ-EDDnp, hereafter named KK-Q) (Fig. 1). The superposition integral (Eq. 1) was calculated in the various experimental conditions described in this work. In the experiments we also measured the refractive index *n* and the quantum yield Φ_d, for the calculation of the Forster distance R_0 in phosphate buffer, in buffer solution containing heparin or SDS micelles, and in buffer/TFE mixtures (Table 1). Fast movement of both donor and acceptor groups was assumed during the excited state lifetime, so that the orientational parameter κ^2 was set equal to 2/3. This assumption was on the basis of time-resolved fluorescence anisotropy results presented by Pimenta and co-workers [36]. An estimate for the error under such assumption was made by Kulinski et al. [32] in the galanin peptide labeled with DNS or DNP as acceptor of the energy transferred from the tryptophan residue, where deviations in Ro could amount to circa 20 %. The lifetime of *o*-Abz is considerably longer than tryptophan and the number of configurations spanned by the donor and acceptor groups is higher, so that we estimate circa 10 % deviation in the calculated values of R_o.

Time-Resolved Fluorescence of Donor

Due to donor to acceptor energy transfer, fluorescence emission decay of internally quenched peptides becomes faster, compared to the decay of the peptide without acceptor (Fig. 2). The decay of the donor group, represented in this work by the peptide KK-A, in phosphate buffer (curve d of Fig. 2) is best fitted to a bi-exponential curve, dominated by a lifetime of 8.6 ns with normalized pre-exponential factor 0.83 (Table 2), responsible for more than 93 % of the total fluorescence emission. The best fit to the experimental curve includes a shorter lifetime of 3.1 ns, which accounts for 7 % of the total emission. As verified by Takara et al. [28], two rotamers can be stabilized, in derivatives of *o*-Abz, which differ by 180° rotation of carboxyl group around its bond to the benzyl ring. Average lifetime, calculated from the usual definition of mean values, is equal to 8.2 ns.

When heparin or SDS micelles are added to the buffer solution both long and short lifetimes presented a small increase, and in SDS the fit included a fast component, lower than 1.0 ns. Similar observation was verified in the decay of the peptide in TFE, and in the presence of heparin or SDS the calculated mean lifetimes increased, compared to the value obtained in buffer (Table 2).

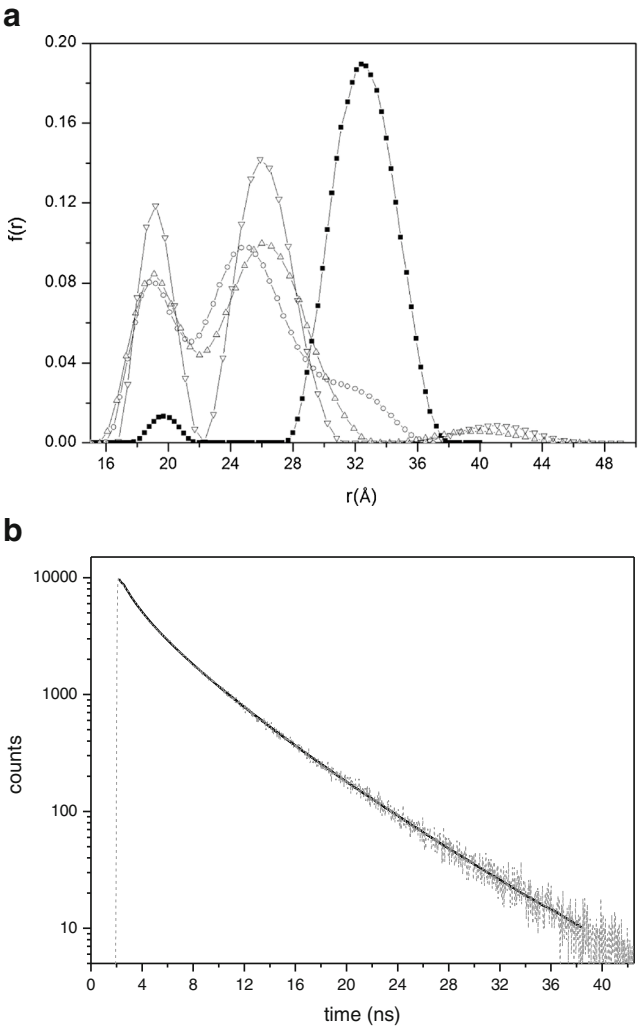

Fig. 4 (**a**) End-to-end distance distributions recovered from intensity decays for the peptide RKK-3 (concentration around 30 μM) in interaction with heparin. Ratio heparin/peptide concentration: 0.00 (*black square*), 0.83 (*white circle*), 1.02 (*white up-pointing triangle*) e 1.44 (*white down-pointing triangle*). (**b**) Fluorescence decay curve (*dashed line*) for RKK-3 peptide 30 μM in phosphate buffer solution pH 7.4 containing equimolar concentration of heparin and fit (*solid line*) to the distance distribution model using the CONTIN program

Heparin-RKK-3 Interaction

The presence of heparin has small effect in the lifetimes for the donor (KK-A) as observed in Table 2. The superposition integral J was determined for several concentrations of heparin added to a solution containing 30 μM of the peptide. The values remained in the interval between 4.85 and 5.13× 10^{-11} M^{-1} cm^3 and the Forster distance fluctuates around 25.8±0.4 Å (Table 3).

The most striking feature of the fluorescence decay of internally quenched peptide is the fastening promoted by energy transfer between the donor group, *o*-Abz, and the acceptor EDDnp, as can be seen comparing curve (a) and curve (d) in Fig. 2. We analyzed the experimental decay under

Table 4 Position of peaks of end-to-end distance distribution (P_i), full width at half maximum (L_i) and relative population (A_i) of the distributions for RKK-3 in interaction with heparin. Ch/Cp – heparin-peptide concentration relation. From the fit using CONTIN, deviations are 0.5 Å in the distances and 0.01 in the relative populations. The sum of relative populations is not 1.0, when there are contributions from short distances

Ch/Cp	P_1 (Å)	P_2 (Å)	L_1 (Å)	L_2 (Å)	A_1	A_2
0.00	19.7	32.4	2.1	5.1	0.03	0.97
0.15	18.7	28.9	3.3	4.8	0.17	0.83
0.47	17.8	24.0	3.0	4.3	0.32	0.54
0.65	18.6	24.9	4.2	6.7	0.38	0.62
0.83	18.8	24.7	4.1	6.8	0.19	0.71
1.02	19.1	26.0	4.1	6.5	0.34	0.63
1.44	19.2	25.9	2.8	4.3	0.33	0.62

the assumption that the distance between donor and acceptor is not fixed, as is usually found in peptides in aqueous medium. The CONTIN program was used to recover a distance distribution *f(r)* from the decay curve, without any a priori hypothesis concerning the distances *r* or the shape of the distribution curves. In buffer solution, pH 7.4, we obtained an end-to-end distance distribution centered at 32.4 Å, and a small population (3 %) of peptides with shorter end-to-end distances, near to 20 Å. Some contribution of very long or very short distances also were recovered however as the distances are larger than $2R_o$ or shorter than *Ro/2* they are hardly discerned from experimental deviations in the decay profiles. From molecular modeling simulations using HyperChem software (Hypercube Inc., Gainesville, FL, U.S.A., http://www.hyper.com), it could be estimated end-to-end distances as large as 90 Å (Fig. 3) for the peptide RKK-3 in extended all trans conformation and the results indicate that the peptide is structured in a more compact conformation.

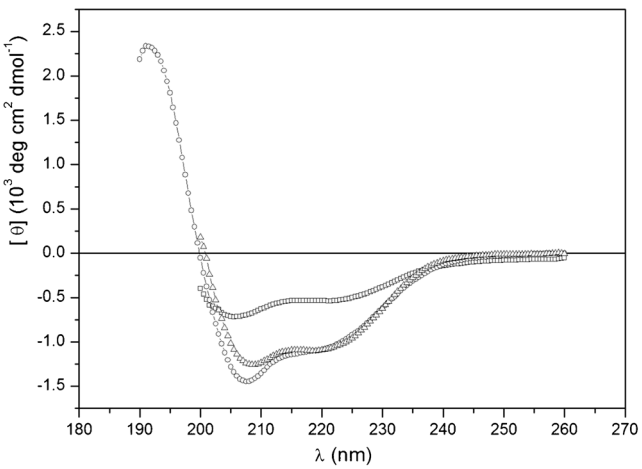

Fig. 5 Circular dichroism spectra of RKK-3 peptide 30 μM in phosphate buffer solution pH 7.4 containing equimolar concentration of heparin (*white square*) or SDS 30 mM (*white up-pointing triangle*). Also shown spectra measured in TFE (*white circle*)

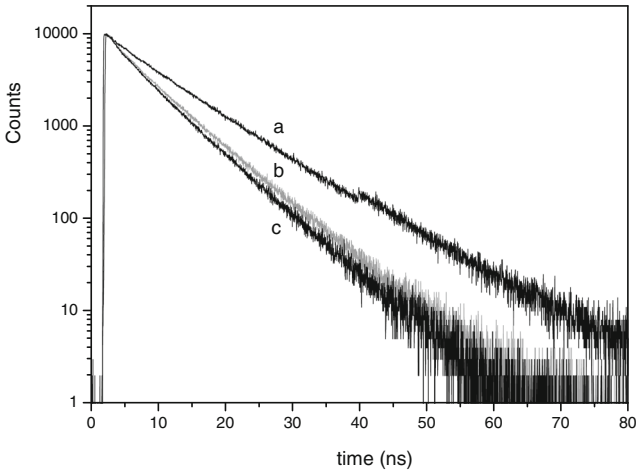

Fig. 6 Fluorescence decay curves for (*a*) KK-A peptide 30 μM in 40 % TFE/water, RKK-3 peptide 30 μM in (*b*) 40 % TFE/water and (*c*) 100 % TFE/water

When heparin is present in the medium the fluorescence intensity decay becomes faster, as seen by comparison of curves (a) and (c) in Fig. 2. The interaction of RKK-3 with heparin promotes conformational changes, shortening the length of the peptide, reflected by the fastening of the intensity decay. When heparin is added in concentrations between 5.0 μM to 40.0 μM (or heparin:peptide molar ratio between 0.15:1.0 and 1.4:1.0), the distance distribution recovered using CONTIN reveals the presence of two main populations, centered typically around 19 and 25 Å (Fig. 4 and Table 4). As cited above, in the fluorescence intensity decay very short component with large deviation was also observed, originating the recovery of short distances in the distribution, below $R_o/2$, inadequate to be considered in FRET formalism. Circular dichroism spectra of the peptide in buffer solution are indicative of a transition from random coil to α-helix secondary structure due to interaction with heparin (Fig. 5). As the end-to-end distances obtained here are shorter than estimated for RKK-3 in α-helix conformation (around 39 Å) (Fig. 3), the results suggest that the heparin molecule also has structural modifications in order to assume more compact conformation. However, alternative heparin conformations that may wrap around the a-helix to facilitate a greater number of ionic contacts with the peptide are energetically unfavorable [20]. Circular dichroism spectra of the peptide in buffer solution indicated increased degree of α-helicity due to interaction with heparin, however in lower extent compared to the result in TFE (Fig. 5). Thus the distances recovered are representative of peptides only partially arranged in α-helix after interaction with heparin.

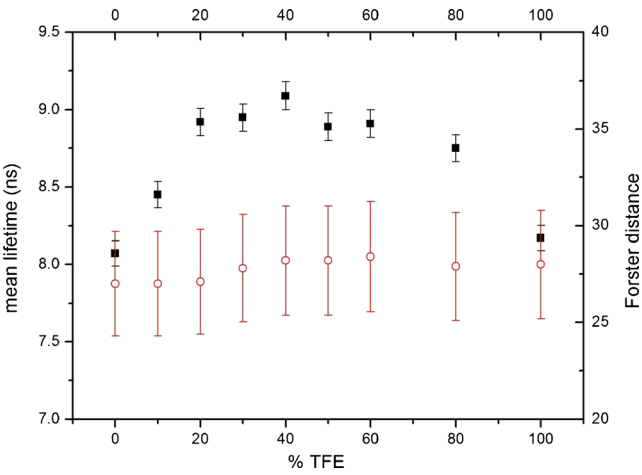

Fig. 7 Fluorescence parameters obtained at several TFE:water volume ratios: (*black square*) mean lifetime of KK-A calculated from intensity decay curves; (*white circle*) Förster distance (Å) calculated for the donor-acceptor pair

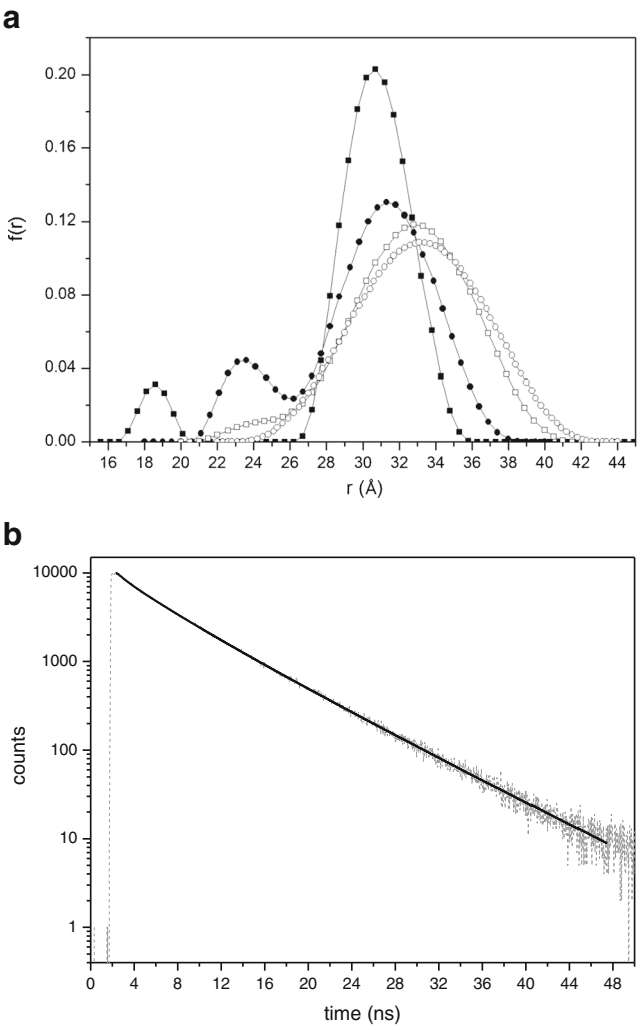

Fig. 8 (**a**) Distance distribution recovered from intensity decay profiles of RKK-3 in TFE:water (%) mixtures using CONTIN. 0 % TFE (*black square*), 20 % TFE (*black circle*), 40 % TFE (*white square*) and 100 % TFE (*white circle*).(*white down-pointing triangle*). (**b**) Fluorescence decay curve (*dashed line*) for RKK-3 peptide 30 μM in TFE and fit (*solid line*) to the distance distribution model using the CONTIN program

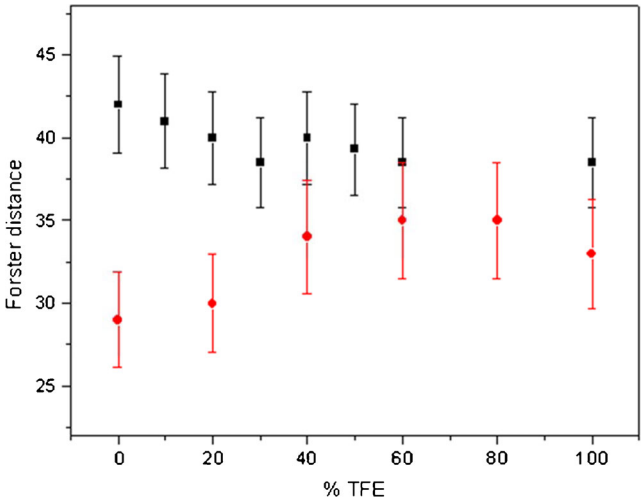

Fig. 9 Peak position of the distance distribution recovered from fluorescence decay of RKK-3 (*white circle*) and RKK-4 (*black square*) in TFE: water mixtures

RKK-3 and RKK-4 in TFE

TFE is a solvent known as inductor of α-helix in peptides, for the hydrophobic groups of TFE can associate with each other, and with the hydrophobic groups of peptide residues [40]. The stabilization of hydrophobic clusters leads to the stabilization of intramolecular hydrogen bonds, to the detriment of the intermolecular H-bonds with water. The intensity decay of KK-A, the peptide labeled with *o*-Abz without the acceptor group, was examined in several TFE:water volume ratio (Fig. 6). The mean lifetime gradually increased with increase in TFE content, attaining a maximum value of 9.05 ns at 40 % TFE (Fig. 7), a volume ratio where the peptide experiences an environment with predominance of TFE. From that point, with further addition of TFE the water molecules are continuously excluded from the neighborhood of the peptide and at 100 % TFE the lifetime decreases to 8.2 ns (Fig. 7). A more pronounced decrease in lifetime, to 5.4 ns, for the isolated probe *o*-Abz in TFE was previously reported [27]. However the derivative with methylated amino, *o*-Abz-$NHCH_3$, presented lifetime value around 8.0 ns in TFE [28], stressing the role of hydrogen bond involving the carboxy and amino groups of the probe. In fact, in the methylated compound, or in Abz-peptides, the amino nitrogen has decreased possibility to do hydrogen bond with the solvent, and intra-molecular hydrogen bond is favoured, stabilizing the excited state and increasing the mean lifetime [28].

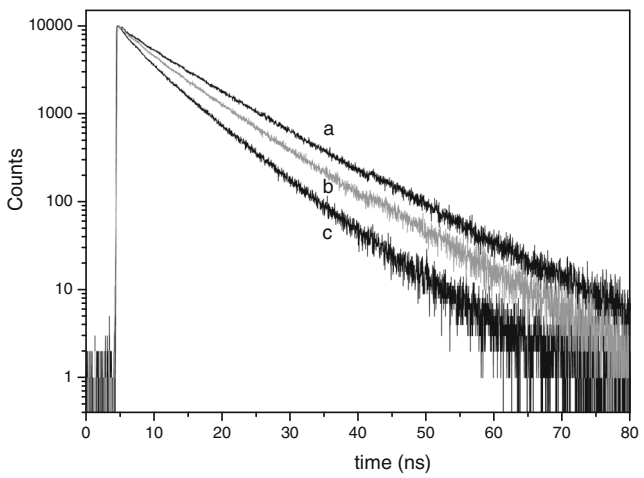

Fig. 10 Fluorescence decay curves for (*a*) KK-A, (*b*) RKK-4 and (*c*) RKK-3 peptides 30 μM in SDS

The propensity of α-helix formation due to interaction with heparin was already reported for RKK-4 peptide [36] and circular dichroism spectra of RKK-3 in TFE confirms the occurrence of the α-helix conformation in the shorter peptide (Fig. 5). Fluorescence experiments were performed in internally quenched RKK-3 (Fig. 6) and RKK-4 in water/TFE

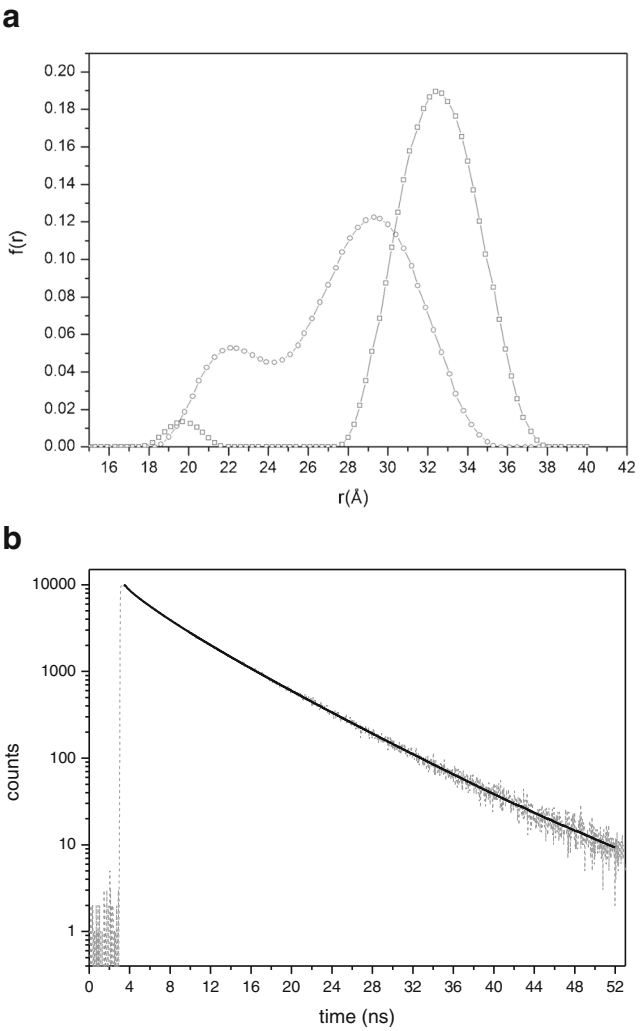

Fig. 11 (**a**) Distance distribution recovered from intensity decay profiles, using CONTIN, for RKK-3 in phosphate buffer pH 7.4 (*white square*), and in buffer solution containing 30 mM SDS (*white circle*). (**b**) Fluorescence decay curve (*dashed line*) for RKK-3 peptide 30 μM in SDS 30 mM and fit (*solid line*) to the distance distribution model using the CONTIN program

mixtures. The values of refractive index, quantum yield, lifetime and superposition integral were determined in each TFE: water volume ratio, and the values of the calculated Förster distances remained between 26 Å and 28 Å (Fig. 7). The intensity decay curves were analyzed using CONTIN, and the recovered distance distribution for RKK-3 showed that the population with end-to-end distances below 24 Å gradually disappeared and above 40 % volume TFE the distribution stabilized around a single peak centered at 33 Å (Fig. 8). This distance should correspond to the α-helix conformation observed in CD spectrum measured in TFE (Fig. 5). The same FRET experiment was conducted with the peptide RKK-4 in water/TFE mixtures and above 40 % TFE, the end-to-end distance recovered using CONTIN also stabilized in a single distribution around 38 Å (Fig. 9). The values are compatible with expected end-to-end distances for α-helix conformation of the peptides, estimated from molecular modeling simulations using HyperChem software.

RKK-3 and RKK-4 in Interaction with SDS Micelles

According to previous reports, *o*-Abz labeled peptides interact with amphiphilic aggregates, and lifetimes above 8 ns were observed in the presence of SDS micelles [29, 31]. We observed that the emission from the KK-A peptide is sensitive to the presence of anionic amphiphilc aggregates. When the surfactant SDS is added in concentration above its CMC, the fluorescence decay of KK-A micelles in phosphate buffer has a long lifetime close to 10.0 ns as the main component. The decay profile is best fitted with the inclusion of an intermediate lifetime of 4.56 ns, and a short component of 0.37 ns (Table 2), and the calculated mean lifetime was 9.25 ns.

From fluorescence parameters of the peptides labeled with donor only or with acceptor only, Forster distances in the presence of SDS micelles were calculated as 25.4 Å (Table 1). As expected, the internally quenched peptides RKK-3 and RKK-4 decay faster than non-quenched KK-A (Fig. 10), and the curves, fitted to tri-exponential decay present mean lifetimes below 8.0 ns in the presence of SDS. The intensity decay curves were analyzed using CONTIN, and the recovered distance distribution for RKK-3 showed that the presence of two populations, the less populated with end-to-end distance centered in 22 Å and the most populated (79 % of the total) centered in 29 Å (Fig. 11). Two populations were also recovered for RKK-4 in SDS, the most populated (84 %) with distances around 28 Å and the other at 44 Å. The CD spectra of both peptides measured in the presence of SDS (as shown in Fig. 5 for RKK-3) are characteristic of α-helix conformation, and should correspond to the long distance populations described here. The minor population with short distances represents compact arrangement stabilized by the electrostatic interactions with the anionic surfactant.

Conclusions

Cardin motif peptides RKK-3 and RKK-4 labeled with the donor group *o*-Abz and the acceptor EDDnp can be conveniently examined within the framework of Förster resonant energy transfer process. The distance distribution recovered from experimental fluorescence decay profiles show that in phosphate buffer RKK-3 peptides are not in *all trans* extended conformation for the end-to-end distances obtained are considerably shorter than expected from elementar modeling simulations.

Gradual addition of low molecular weight heparin (15 kD) promotes shortening of donor-acceptor distances, and at concentrations around equimolar peptide/heparin ratio, we have two populations of peptides, one (65 % populated) with end-to-end distances around 26 Å and the other (35 % populated) around 19 Å. The results obtained for RKK-3 are in agreement with previous observations with peptides RKK-4 and KK-4.

The formation of α-helix secondary structure was evaluated in water/TFE mixtures. The time-resolved florescence decay of the reference peptide KK-A, as well as the values of the Förster distances showed gradual modifications with increase in TFE content of mixtures, attaining a maximum at 40 % TFE/water volume ratio. At this ratio the α-helix is stabilized and the donor-acceptor distances in internally quenched peptides are described by a single population with end-to-end distances centered in 33 Å in RKK-3 and 38 Å in RKK-4. The correspondence with α-helix structure is ascertained by CD spectra of the peptides, and the results show that in the interaction with heparin additional turning in the glycosaminoglycan promotes decrease in the end-to-end distance.

The interaction with SDS anionic micelles stress the importance of electrostatic effects in the interaction. Like heparin, the anionic surfactant organized in micellar aggregates promotes arrangements of peptides in two populations. The combination of electric interactions and hydrogen bond formation results in structuration as α-helix, and additional shortening of end-to-end distances of RKK-3 and RKK-4.

Acknowledgments We thank the Brazilian agencies FAPESP, CNPq and FAPESP projeto temático 12/50191-4 for financial support. Support from INCT-FCx, Brazil, is also acknowledged.

References

1. Jackson RL, Busch SJ, Cardin AD (1991) Glycosoaminoglycans: molecular properties, protein interactions, and role in physiological processes. Physiol Rev 71:481–529
2. Lane DA, Denton J, Flynn AM, Thunberg L, Lindahl U (1984) Anticoagulant activities of heparin oligosaccharides and their neutralization by platelet factor 4. Biochem J 218:725–732
3. Olson ST, Bjork I, Sheffer R, Craig PA, Shore JD, Choay J (1992) Role of the antithrombin-binding pentasaccharide in heparin

acceleration of antithrombin proteinase reactions. Resolution of the antithrombin conformational change contribution to heparin rate enhancement. J Biol Chem 267:12528–12538
4. Jin L, Abrahams JP, Skinner R, Petitou M, Pike RN, Carrell RW (1997) The anticoagulant activation of antithrombin by heparin. Proc Natl Acad Sci U S A 94:14683–14688
5. Chuang YJ, Swanson R, Raja SM, Olson ST (2001) Heparin enhances the specificity of antithrombin for thrombin and factor Xa independent of the reactive centre loop sequence. Evidence for an exosite determinant of factor Xa specificity in heparin-activated antithrombin. J Biol Chem 276:14961–14971
6. Choay J, Lormeau JC, Petitou M, Sinay P, Fareed J (1981) Structural studies on a biologically active hexasaccharide obtained from heparin. Ann N Y Acad Sci 370:644–649
7. Pixley R, Danishefsky I (1982) Preparation of highly stable antithrombin-sepharose and utilization for the fractionation of heparin. Thromb Res 26:129–133
8. Höök M, Björk I, Hopwood J, Lindahl U (1976) Anticoagulant activity of heparin: separation of high-activity and low-activity heparin species by affinity chromatography on immobilized antithrombin. FEBS Lett 66:90–93
9. Racanelli A, Fareed J, Walenga JM, Coyne E (1985) Biochemical and pharmacologic studies on the protamine interactions with heparin, its fractions and fragments. Semin Thromb Hemost 11:176–189
10. DeLucia A, Wakefield TW, Andrews PC, Nichol BJ, Kadell AM, Wrobleski SK, Downing LJ, Stanley JC (1993) Efficacy and toxicity of differently charged polycationic protamine-like peptides for heparin anticoagulation reversal. J Vasc Surg 18:49–60
11. Schick BP, Gradowski JF, San Antonio JD, Martinez J (2001) Novel design of peptides to reverse the anticoagulant activities of heparin and other glycosaminoglycans. Thromb Haemost 85:482–487
12. Schick BP, Maslow D, Moshinski A, San Antonio JD (2004) Novel concatameric heparin-binding peptides reverse heparin and low-molecular-weight heparin anticoagulant activities in patient plasma in vitro and in rats in vivo. Blood 103:1356–1363
13. Liu S, Zhou F, Höök M, Carson DD (1997) A heparin-binding synthetic peptide of heparin/heparan sulfate-interacting protein modulates blood coagulation activities. Proc Natl Acad Sci U S A 94: 1739–1744
14. Wang J, Rabenstein DL (2006) Interaction of heparin with two synthetic peptides that neutralize the anticoagulant activity of heparin. Biochemistry 45:15740–15747
15. Verrecchio A, Germann MW, Schick BP, Kung B, Twardowski T, San Antonio JD (2000) Design of peptides with high affinities for heparin and endothelial cell proteoglycans. J Biol Chem 275:7701–7707
16. Cardin AD, Weintraub HJR (1989) Molecular modeling of protein-glycosaminoglycan interactions. Arterioscler Thromb Vasc Biol 9:21–32
17. Montserret R, Aubert-Foucher E, McLeish MJ, Hill JM, Ficheux D, Jaquinod M, van der Rest M, Deléage G, Penin F (1999) Structural analysis of the heparin-binding site of the NC1 domain of collagen XIV by CD and NMR. Biochemistry 38:6479–6488
18. Ringstad L, Schmidtchen A, Malmsten M (2006) Effect of peptide length on the interaction between consensus peptides and DOPC/DOPA bilayers. Langmuir 22:5042–5050
19. Capila I, Linhardt RJ (2002) Heparin-protein interactions. Angew Chem Int Ed 41:390–412
20. Rullo A, Nitz M (2009) Importance of spatial display of charged residues in heparin-peptide interactions. Biopolymers 93:290–298
21. Remko M, Van Duijnen PT, Broer R (2013) Structure and stability of complexes of charged structural units of heparin with arginine and lysine. RSC Adv 3:1789–1796
22. Gershkolovich AA, Kholodovich VV (1996) Fluorogenic substrates for proteases based on intramolecular fluorescence energy transfer (IEFTS). J Biochem Biophys Methods 33:135–162
23. Knight CG (1995) Fluorometric assays of proteolytic enzymes. Methods Enzymol 248:18–34
24. Chagas JR, Portaro FC, Hirata IY, Almeida PC, Juliano MA, Juliano L, Prado ES (1995) Determinants of the unusual cleavage specificity of lysyl-bradykinin-releasing kallikreins. Biochem J 306:63–69
25. Del Nery E, Chagas JR, Juliano MA, Prado ES, Juliano L (1995) Evaluation of the extent of the binding site in human tissue kallikrein by synthetic substrates with sequences of human kininogen fragments. Biochem J 312:233–238
26. Ito AS, Turchiello RF, Hirata IY, Cezari MH, Meldal M, Juliano L (1998) Fluorescent properties of amino acids labeled with orthoaminobenzoic acid. Biospectroscopy 4:395–402
27. Takara M, Ito AS (2005) General and specific solvent effects in optical spectra of *ortho*-aminobenzoic acid. J Fluoresc 15:171–177
28. Takara M, Eisenhut JK, Hirata IY, Juliano L, Ito AS (2009) Solvent effects in optical spectra of *ortho*-aminobenzoic acid derivatives. J Fluoresc 19:1053–1060
29. Turchiello RF, Lamy-Freund MT, Hirata IY, Juliano L, Ito AS (1998) *Orto*-aminobenzoic acid as a fluorescent probe for the interaction between peptides and micelles. Biophys Chem 73:217–225
30. Ray R (1993) Fluorescence quenching of o-Aminobenzoic acid by ethylene trithiocarbonate in aqueous micellar media. J Photochem Photobiol A 76:115–120
31. Turchiello RF, Lamy-Freund MT, Hirata IY, Juliano L, Ito AS (2002) *Ortho*-aminobenzoic acid labeled bradykinins in interaction with lipid vesicles: a fluorescence study. Biopolymers 65:336–346
32. Kulinski T, Wennerberg AB, Rigler R, Provencher SW, Pooga M, Langel U, Bartfai T (1997) Conformational analysis of galanin using end to end distance distribution observed by Forster resonance energy transfer. Eur Biophys J 26:145–154
33. Souza ES, Hirata IY, Juliano L, Ito AS (2000) End-to-end distribution distances in bradykinin observed by fluorescence energy transfer. Bioch Biophys Acta 1474:251–261
34. Ito AS, Souza ES, Barbosa SR, Nakaie CR (2001) Fluorescence study of conformational properties of melanotropins labeled with aminobenzoic acid. Biophys J 81:1180–1189
35. Montaldi LR, Berardi M, Souza ES, Juliano L, Ito AS (2012) End-to-end distance distribution in fluorescent derivatives of bradykinin in interaction with lipid vesicles. J Fluoresc 22:1151–1158
36. Pimenta DC, Nantes IL, Souza ES, Le Bonniec B, Ito AS, Tersariol ILS, Oliveira V, Juliano MA, Juliano L (2002) Interaction of heparin with internally quenched fluorogenic peptides derived from heparin-binding consensus sequences, kallistatin and anti-thrombin III. Biochem J 366:435–446
37. Hirata YI, Cezari MHS, Nakaie CR, Boschcov P, Ito AS, Juliano MA, Juliano L (1994) Internally quenched fluorogenic protease substrates: solid-phase synthesis and fluorescence spectroscopy of peptides containing ortho-aminobenzoyl/dinitrophenyl groups as donor-acceptor pairs. Lett Pept Sci 1:299–308
38. Melhuish WH (1961) Quantum efficiencies of fluorescence of organic substances: effect of solvent and concentration of the fluorescent solute. J Phys Chem 65:229–235
39. Provencher SW (1982) CONTIN: a general purpose constrained regularization program for inverting noisy linear algebraic and integral equations. Comput Phys Commun 27:229–242
40. Hirota N, Mizuno K, Goto Y (1998) Group additive contributions to the alcohol-induced α-helix formation of melittin: implication for the mechanism of the alcohol effects on proteins. J Mol Biol 275:365–378